New Phytologist

Research

Precipitation, solar radiation, and their interaction modify leaf hydraulic efficiency–safety trade-off across angiosperms at the global scale

Yi Jin[1,2], Qing Ye[1], Xiaorong Liu[3], Hui Liu[1,2], Sean M. Gleason[4], Pengcheng He[1], Xingyun Liang[1] and Guilin Wu[5]

[1]Guangdong Provincial Key Laboratory of Applied Botany, Key Laboratory of National Forestry and Grassland Administration on Plant Conservation and Utilization in Southern China, South China Botanical Garden, Chinese Academy of Sciences, Guangzhou, 510650, China; [2]Jiangxi Provincial Key Laboratory of Carbon Neutrality and Ecosystem Carbon Sink, Lushan Botanical Garden, Chinese Academy of Sciences, Jiujiang, 332900, China; [3]The Research Center for the Development of Sichuan Old Revolutionary Area, Sichuan University of Arts and Science, Dazhou, 635000, China; [4]Water Management and Systems Research Unit, USDA-ARS, Fort Collins, CO 80526, USA; [5]Hainan Jianfengling Forest Ecosystem National Field Science Observation and Research Station, Research Institute of Tropical Forestry, Chinese Academy of Forestry, Guangzhou, 510520, China

Author for correspondence:
Qing Ye
Email: qye@scbg.ac.cn

Received: *12 June 2024*
Accepted: *28 September 2024*

New Phytologist (2024)
doi: 10.1111/nph.20213

Key words: angiosperms, biome, climatic factors, leaf functional traits, leaf hydraulic efficiency, leaf hydraulic safety, trade-off.

Summary

- In theory, there is a trade-off between hydraulic efficiency and safety. However, the strength and direction of this trade-off at the leaf level are not consistent across studies, and habitat climate may impact this trade-off.
- We compiled a leaf hydraulic efficiency and safety dataset for 362 species from 81 sites world-wide, with 280 paired observations of both traits, and tested whether climate was associated with departure from the proposed trade-off.
- The leaf hydraulic efficiency–safety trade-off was weak (R^2 = 0.144) at the global scale. Mean annual precipitation and solar radiation (SR) modified the trade-off. Species from dry and high SR habitats (e.g. desert and tropical savanna) were generally located above the trade-off line, indicating that these species tended to have higher leaf hydraulic safety and efficiency than species from wet habitats with low SR (e.g. subtropical monsoon forest and montane rainforest), which were located below the trade-off line. Leaves with high vein density, dry leaf mass per area, and osmotic regulation enhanced safety without compromising hydraulic efficiency.
- Variation in the hydraulic efficiency–safety trade-off at the leaf level likely facilitates plant survival in specific habitats and allows for a more nuanced view of leaf hydraulic adaption strategies at the global scale.

Introduction

Identifying trade-offs is necessary for understanding trait variation and ecological strategies across species and habitats (Reich, 2014). A well-known eco-physiological theory proposes that there should be a trade-off between a plant's capacity to transport water (hereafter: 'hydraulic efficiency') and a plant's resistance to hydraulic failure at low water potential (hereafter: 'hydraulic safety') (Zimmermann, 1983; Ocheltree *et al.*, 2016). This hypothesis has been widely tested on branches/stems, and a significant but weak trade-off has been found at the global scale (Gleason *et al.*, 2016; Liu *et al.*, 2021). Possible mechanisms underpinning this trade-off are thought to arise from the anatomical and biophysical characteristics of xylem (Bittencourt *et al.*, 2016; Brodersen, 2016; Gleason *et al.*, 2016). Meanwhile, it has been suggested that seasonal climate factors would likely modify the trade-off (Liu *et al.*, 2021). However, research investigating the trade-off at the leaf level has received far less attention than investigations focused on branches and stems.

Leaves, at the end of the plant water transport pathway, contribute > 30% to whole plant resistance, and are thus considered an important hydraulic 'bottleneck' (Sack & Frole, 2006; Sack & Holbrook, 2006). Leaf hydraulic efficiency (the maximum leaf hydraulic conductance (K_{leaf}), K_{max}), which is strongly and causally related to photosynthetic capacity (Brodribb *et al.*, 2007; Scoffoni *et al.*, 2016), reflects xylem characteristics (e.g. lumen, pit, and pit membrane resistances), xylem network connectivity, and resistances associated with liquid phase transport between the vein endings and the sites of evaporation (hereafter: 'extraxylary' resistance). Leaf hydraulic safety, which is usually estimated by the leaf water potential resulting in a 50% decline from K_{max} (P_{50}), reflects xylem embolism and conduit collapse resistances, as well as declines in plasma membrane permeability/integrity and the loss of cell turgor, which are associated with the ability of a plant to maintain gas exchange at low water potential (Blackman *et al.*, 2012; Scoffoni & Sack, 2017). Studies investigating the trade-off between $K_{\max}$ and P_{50} have yielded inconsistent results. For example, the trade-off was not found in several regional studies (Blackman *et al.*, 2010; Scoffoni *et al.*, 2011a; Bucci *et al.*, 2013; Yao *et al.*, 2021; Zhang *et al.*, 2021; Xiong & Flexas, 2022), as well as an across-region study of 130 species (Nardini & Luglio, 2014). By contrast, Scoffoni & Sack (2017) and Yan *et al.* (2020) found evidence for a safety–efficiency trade-off across 137 species and 311 species, respectively. Strong safety–efficiency trade-offs have also been reported across smaller numbers of species (Ocheltree *et al.*, 2016; Bucci *et al.*, 2019; Huo *et al.*, 2022; Zhang *et al.*, 2024). It is possible that anatomical and climatological factors may be responsible for these conflicting results, and further study in these areas may improve our understanding of safety–efficiency relationships.

Some studies have shown that both xylem and extraxylary characteristics of leaves appear to be aligned with the existence of a trade-off. Water transport through leaf xylem must pass through the same anatomical features found in branch and stem xylem, for example conduits and inter-conduit pit membranes, that influence both hydraulic efficiency and safety (Gleason *et al.*, 2016; Scoffoni *et al.*, 2017; Blackman *et al.*, 2024). At the scale of whole vascular bundles, it is thought that vein width is related to network conductivity positively (McKown *et al.*, 2010), but drought stress negatively (Brodribb *et al.*, 2016). High irradiance enhances extraxylary conductance (Sack *et al.*, 2005), but leaf hydraulic conductance under this condition may also be more vulnerable to dehydration (lower safety) (Trifilò *et al.*, 2021), which indicates that a component of extraxylary conductance may be positively aligned with leaf hydraulic efficiency but negatively aligned with hydraulic safety. Researchers have found that leaves with higher leaf mass per unit area (LMA) were associated with low leaf hydraulic conductance, possibly arising from thicker leaves requiring longer extraxylary pathlengths (Nardini *et al.*, 2012, 2014; Buckley *et al.*, 2015; Zhang *et al.*, 2024). Meanwhile, denser leaves (in contrast to thicker leaves) would also result in higher LMA, but would serve to slow down leaf shrinkage and increase leaf hydraulic safety (Nardini *et al.*, 2012, 2014; Scoffoni *et al.*, 2014; Buckley *et al.*, 2015; John *et al.*, 2017; Zhu *et al.*, 2018). However, it is also becoming clear that xylem and extraxylary features conferring hydraulic efficiency vs hydraulic safety are not always the same. For example, some researchers have suggested that hydraulic safety is mainly aligned with the properties of bordered pit membranes, nano-bubble stabilization, and liquid–gas interactions at the conduit/pit surfaces rather than conduit diameters (Lens *et al.*, 2011, 2022; Schenk *et al.*, 2015, 2018), although this idea has yet to be tested across a large number of species (Isasa *et al.*, 2023). Higher vein density (VD) (including both minor and major VD) is associated with higher xylem network connectivity and $K_{\max}$ (Sack & Scoffoni, 2013; Buckley *et al.*, 2015; Yao *et al.*, 2021). It is thought that higher VD and network connectivity provide alternative routes around embolized network sections and thus increase hydraulic safety (Sack *et al.*, 2008, 2013; Scoffoni *et al.*, 2011b; Nardini *et al.*, 2012). Similarly, thicker leaves with higher LMA may provide more alternative extraxylary routes for water transport (Sack *et al.*, 2013), as supported by a positive relationship between $K_{\max}$ and LMA (Xiong *et al.*, 2014). What is more, in contrast with branches and stems, leaves are less expensive organs that can be dropped when necessary to protect branches from desiccation, and thus help plants escape drought (Grubb, 1998; Tyree & Zimmermann, 2002), which can alleviate a plant's requirement for high safety. Therefore, there are no reasons to necessarily expect an unavoidable trade-off between leaf hydraulic efficiency and safety.

Beyond the physiological reasons, we also might expect climate to affect the trade-off between leaf hydraulic efficiency and safety. Given that $K_{\max}$ and P_{50} relate to strategies of growth and survival, many studies have shown that species growing in wetter regions with higher mean annual precipitation (MAP) and/or warmer regions with higher mean annual temperature (MAT), such as tropical forests, to have higher efficiency (Sack & Holbrook, 2006; Nardini & Luglio, 2014). In support of this idea, species from similar climates as these have been reported to have lower levels of safety (higher P_{50}) (Blackman *et al.*, 2012, 2014; Nardini & Luglio, 2014; Scoffoni & Sack, 2017). However, in contrast with these reports, a recent study has shown that plants in arid regions not only have higher safety, but also have greater efficiency (Yao *et al.*, 2021), and some researchers have found that species have higher safety but no significant difference in efficiency between dry and moist habitats (Scoffoni *et al.*, 2011a). Similarly, $K_{\max}$ and P_{50} have been found to vary independently with the distribution of species across precipitation or temperature gradients (Ocheltree *et al.*, 2016; Huang *et al.*, 2024). Indeed, a high capacity for leaf water transportation may provide plants additional survival advantages: (1) higher efficiency mitigates the greater evaporative load and reduces the pressure gradient in leaves that arise from high evaporative demand, that is high vapor–pressure deficit (VPD) environments; (2) the latent heat flux associated with transpiration serves to reduce leaf temperature; (3) high efficiency allows for high rates of gas exchange in intermittently wet/dry habitats when water is readily available (i.e. 'use it or lose it') (Grubb, 1998; Yao *et al.*, 2021; Bi *et al.*, 2023). In contrast to the benefits of high hydraulic efficiency, greater hydraulic safety allows plants to maintain gas exchange and growth when leaf water potential drops significantly and leads a large decline in K_{leaf} and stomatal closure during drought (Holloway-Phillips & Brodribb, 2011; Martorell *et al.*, 2015). Therefore, it is reasonable to assume that safety and efficiency are not tightly coupled by anatomical or biophysical constraints, leaving natural selection free to 'choose' higher/lower levels of efficiency and safety to achieve improved hydraulic functioning in particular habitats. If this is a fair assumption, then we should expect marked departure in the trade-off, and this departure (e.g. improved performance in dimension relative to the other) should be achieved via leaf functional traits (e.g. VD, LMA, and turgor loss point (TLP)). As mentioned previously, species living in highly seasonal climates have higher stem efficiency and safety than species from sites with low seasonality at the global scale (Liu *et al.*, 2021). However, the specific climatic factors associated with departure from the proposed trade-off between leaf hydraulic efficiency and safety are still unclear. Identifying the climate factors aligned with departures from the trade-off would help us understand how leaf hydraulic strategies affect species distributions across climate gradients.

In this study, we compiled a dataset of K_{max} and P_{50}, as well as other related traits, for 362 species from 81 sites world-wide, which included 280 observations of paired measurements of both K_{max} and P_{50}, with the aim of addressing the following questions: (1) How are K_{max} and P_{50} aligned with one another at the global scale, that is how does the strength and direction of the trade-off vary across species, and how well does the unexplained variation in the trade-off align with other leaf functional traits? (2) How does this trade-off vary with climate and across biomes?

Materials and Methods

Data collection

We combined published and unpublished measurements of leaf hydraulic efficiency and safety for angiosperms. Most of these data were collected from previously published studies sourced by searching the Web of Science, Google Scholar, and China National Knowledge Infrastructure (http://www.cnki.net) (see Supporting Information Notes S1). We also extracted data on other leaf functional traits that may influence these two leaf hydraulic traits, when they were available from the same studies. These traits included LMA, pressure-volume curve parameters (modulus of elasticity (ε), osmotic potential at full turgor (π_0), leaf water potential at TLP), VD, major VD, and minor VD (Table 1). Leaf hydraulic efficiency and safety were also measured for 51 species at the Dinghushan Biosphere Reserve in southern China (unpublished data, Liu et al.). Measurements on these 51 species were performed from June to September 2020. Leaf hydraulic conductance (K_{leaf}) and vulnerability to low water potential were measured using the evaporative flux method (EFM) (Sack & Scoffoni, 2012). K_{leaf} was measured on excised leaves that were subjected to a range of water potentials by drying them on a laboratory bench. Two leaves were used to quantify water potential (Ψ_{leaf}), and K_{leaf} was measured on a third leaf from the same twig. K_{leaf} and Ψ_{leaf} were fit with 2-parameter Weibull models using the R package FITPLC (Duursma & Choat, 2017). The maximum value of K_{leaf} (K_{max}) and the leaf water potential at 50% loss of K_{max} (P_{50}) were extracted from these fitted models. Each fitted model (species) consisted of 30–50 observations (leaves) from three to five individual plants. More data were compiled from the literature conforming to the following criteria: (1) Measurements were taken on field plants growing in their natural environment (no pot or common garden experiments). (2) Measurements were conducted on mature plants. We used mean values for each species at the same site (He *et al.*, 2020; Liu *et al.*, 2021). The final data in our study included 362 angiosperm species from 81 sites (Fig. S1a; including 385 observations of K_{max}, 298 observations of P_{50}, and 280 observations of P_{50} and K_{max} measured together; see Dataset S1). We included five different K_{leaf} methods: dynamic rehydration kinetics method (DRKM) (Blackman & Brodribb, 2011), EFM (Sack & Scoffoni, 2012), rehydration kinetics method (RKM) (Brodribb & Holbrook, 2003), pressure bomb method (PBM) (Franks, 2006) and high-pressure flow meter (HPFM) (Sack *et al.*, 2002). Four of these methods were used for P_{50} and trade-off residual determination (all except HPFM). Among these methods, RKM and DRKM accounted for 51% and 28% of the total determinations of residuals, respectively, PBM was used to determine trade-off residuals for only 10 records.

Table 1 List of measured traits, methods of leaf hydraulic conductance used, and all biomes sampled in this study.

Full name	Unit	Symbol
Traits examined in this study		
Maximum leaf hydraulic conductance	mmol m^{-2} s^{-1} MPa^{-1}	K_{leaf}
Leaf water potential at 50% loss of K_{leaf}	MPa	P_{50}
Residual value of standardized major axis regression between K_{leaf} and P_{50}	Unitless	Residuals
Modulus of elasticity	MPa	ε
Osmotic potential at full turgor	MPa	π_0
Turgor loss point	MPa	TLP
Leaf mass per leaf area	g m^{-2}	LMA
Major vein density	mm mm^{-2}	Major VD
Minor vein density	mm mm^{-2}	Minor VD
Vein density	mm mm^{-2}	VD
Mean annual precipitation	mm	MAP
Mean annual temperature	°C	MAT
Precipitation seasonality	Unitless	Ps
Mean annual solar radiation	kJ m^{-2} d^{-1}	SR
Mean annual vapor–pressure deficit	kPa	VPD
Potential evapotranspiration	mm yr^{-1}	PET
Aridity index (MAP/PET)	Unitless	AI
Methods of leaf hydraulic conductance determination		
Dynamic rehydration kinetics method		DRKM
Evaporative flux method		EFM
Rehydration kinetics method		RKM
Pressure bomb method		PBM
High-pressure flow meter method		HPFM
Biomes		
Tropical rainforest		TRR
Tropical savanna		TS
Subtropical monsoon forest		SMF
Montane rainforest		MRF
Temperate deciduous forest		TMD
Woodland and shrubland		WS
Desert		DES

We included seven climate variables that we thought could influence the trade-off (e.g. slope and elevation) based on theory and empirical results (Sack & Holbrook, 2006; Blackman *et al.*, 2014; Nardini & Luglio, 2014; Scoffoni *et al.*, 2016; Scoffoni & Sack, 2017; Yao *et al.*, 2021): MAT, MAP, seasonality of precipitation (Ps; coefficient of variation across monthly measurements × 100), mean annual solar radiation (SR), aridity index (AI), VPD, and potential evapotranspiration (PET). Climate data from each site were acquired from the original literature if available. The remaining climate variables were extracted from WorldClim v.2.1 (http://worldclim.org) (Fick & Hijmans, 2017) and the CGIAR-CSI consortium (http://www.cgiar-csi.org) (Zomer *et al.*, 2008). VPD was calculated as the difference between measured water vapor pressure (VP) and VP at saturation. VP was extracted from the TerraClimate dataset (http://www.climatologylab.org) (Abatzoglou *et al.*, 2018).

We plotted MAT against MAP to obtain Whittaker's biomes classification diagram for all sites included in the dataset (Fig. S1b) (Whittaker, 1975). Study sites were classified as tropical rainforest (TRR), tropical savanna (TS), subtropical monsoon forest (SMF), montane rainforest (MRF), temperate deciduous forest (TMD), woodland and shrubland (WS), and desert (DES) (Fig. S1b). All Whittaker biomes were represented in our dataset except tundra and boreal forest.

Data analysis

The data were log-transformed to meet the assumptions of normality when needed. Absolute values of P_{50}, π_0 and TLP were used given that the original values were negative (Liu *et al.*, 2021). We fit standardized major axis (SMA) models to estimate the trade-off between $K_{\max}$ and P_{50} at the global and regional scales. Residuals from the safety–efficiency SMA fit at global scale were saved as a new variable to represent variation orthogonal to the trade-off (Gleason *et al.*, 2016). These residuals are the difference between the actual observed values and the estimated values and represent the standardized perpendicular distance of each species/observation from trade-off line (departure from proposed trade-off), that is species with more positive/negative residuals have relatively higher/lower level of safety and efficiency, respectively (Gleason *et al.*, 2016; Liu *et al.*, 2021).

We used multiple linear mixed regression modeling (MLMM) to estimate the relative importance of climate factors to predict trade-off residuals, $K_{\max}$, and P_{50}. We treated climate variables as fixed effects and species as random effects. The environmental factors were standardized through z score before analysis, and then, the relative effect of each factor was quantified as the percentage of absolute value of each parameter estimate to the sum of absolute values of all parameter estimates (García-Palacios *et al.*, 2018). We found weak collinearity among the climate factors in our data (Fig. S2; Table S1), that is the variance inflation factor for all predictors was < 10. It became apparent early on in our analyses that SR and MAP explained much of the variation in the trade-off residuals. Thus, we examined the interactive effects of MAP and SR on variation in the trade-off residuals, which was also emphasized by previous studies (Guyot *et al.*, 2012; Trifilò *et al.*, 2021).

We used multiple linear regression to determine whether other leaf traits could account for significant portions of unexplained variation in the $K_{\max}$ and P_{50} trade-off, and also the relative alignment of these traits with $K_{\max}$ and P_{50} individually. This was done by partitioning the regression sum of squares into the independent fractions of variation that were explained by each trade-off variable ($K_{\max}$ or P_{50}) (Gleason *et al.*, 2016). A one-way analysis of variance (ANOVA) was used to compare the trade-off residuals, $K_{\max}$ and P_{50} among biomes. We also calculated the average values of the MAP and SR of the sites in each biome and compared the leaf hydraulic strategies of species living in regions with marked differences in MAP and SR. The distribution of $K_{\max}$, P_{50}, and trade-off residuals across the different biomes in our dataset were expressed using density plots.

Standardized major axis models were fit using the 'sma' function in the R package smatr (Warton *et al.*, 2012). Mixed linear models were fit using the 'lmer' function in the R package lme4 (Bates *et al.*, 2015). Density plots were done using the R package ggplot2 (Wickham, 2016). Variance decomposition was done using the 'lmg' function in the R package relaimpo (Grömping, 2006). All analyses were performed using R software (v.4.3.1).

Results

Leaf hydraulic efficiency and safety were weakly but significantly correlated ($R^2 = 0.144$, $P < 0.001$) (Fig. 1). The multiple linear mixed regression model using seven climate variables explained a total of 18.4% of the variation in the trade-off residuals. MAP and SR were the two main determinants of the trade-off residuals, explaining 32.9% ($P < 0.05$) and 35.3% ($P < 0.001$) of the total explained variation, respectively (Fig. 2). SR also explained much of the variation in P_{50} (35.4%, $P < 0.001$), whereas MAP explained 13.2% ($P < 0.05$) of the total explained variation. Neither of these two climate variables explained significant portions of variation in $K_{\max}$. However, Ps (23.8%; $P < 0.001$), and VPD (22.0%; $P < 0.01$) were significant independent predictors of $K_{\max}$ (Fig. S3a,b).

We found that the trade-off residuals and leaf hydraulic safety decreased with increasing precipitation, but increased with increasing SR (Figs 2, S3b; Tables S2, S3). Species in wet regions (e.g. MAP ≥ 1600 mm) and low SR conditions (e.g. SR $< 10^{4.147}$ kJ m^{-2} d^{-1}) had no significant trade-off and many species from such conditions were located below the trendline (Fig. S4; Tables S4, S5), whereas most species from dry (e.g. MAP < 400 mm) and high SR regions were above the trade-off trendline (Fig. S4). The combination of MAP and SR had interactive effects on the trade-off residuals (MAP × SR: $P < 0.05$) such that the predicted surface was twisted plane, and explained *c.* 16.8% of the variation in trade-off residuals (Fig. 3). When SR was considered in isolation to MAP, it had no significant effect on the trade-off residuals, but altered the effect of MAP on the residuals (Fig. 3). The trade-off residuals decreased slightly with increasing SR, but only in low MAP climates. By contrast, in high MAP climates, trade-off residuals increased with increasing SR. This leverage of MAP on the trade-off residuals resulted in a twisted surface such that the plane was relatively flat across much of the range in both MAP and SR, but then became very steep when MAP was high but SR was low (Figs 3, S5). Plants living in habitats with high SR and low MAP usually had large positive trade-off residuals, whereas plants growing in wet but low SR conditions generally had large negative trade-off residuals (Fig. 3). MAP and SR also had interactive effects on $K_{\max}$ (MAP × SR: $P < 0.001$) but drove P_{50} variation independently

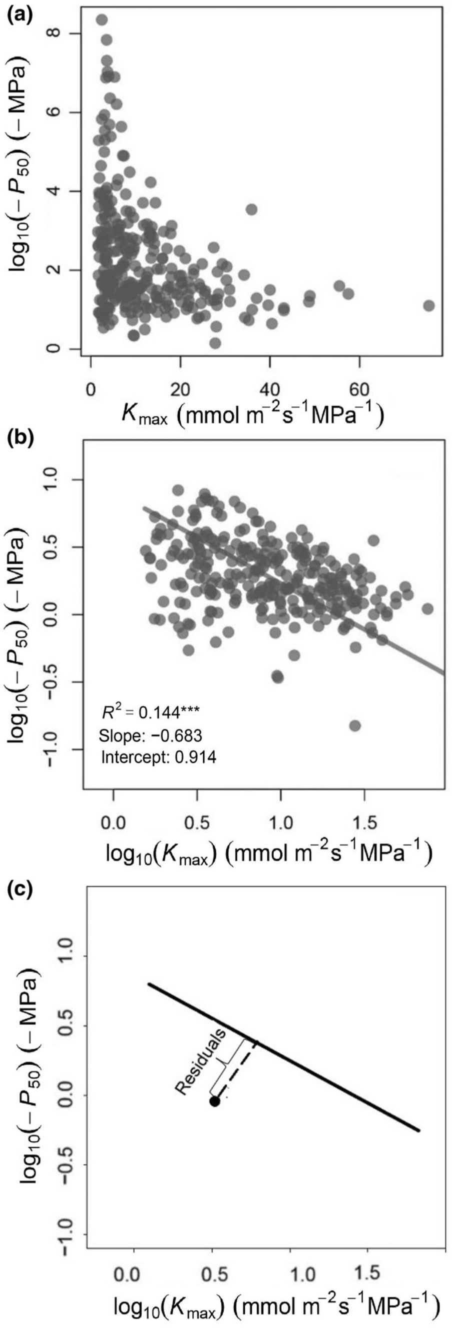

Fig. 1 (a) Leaf hydraulic efficiency (K_{max}) and safety (P_{50}, leaf water potential at a loss 50% K_{max}) plot for all data. (b) K_{max} and P_{50} relationship after being log-transformed and fit with a standard major axis (SMA) model. (c) Schematic diagram of an SMA model residual, representing variation in K_{max} and P_{50} orthogonal to the fitted trendline. Asterisks indicate levels of significance based on the SMA model (***, $P < 0.001$).

(nonsignificant interaction, MAP × SR: $P > 0.05$) and the predicted surface was a plane (Figs S6, S7).

We found that plants in TS, where SR was the highest, and plants from DES sites, where MAP was the lowest, had the largest trade-off residuals. In contrast to this, species from SMF and rainforest sites (MRF and TRR), habitats with high MAP and low SR, had the lowest trade-off residuals (Fig. 4a). Species living in TS had the highest K_{max}, and species from woodland/shrubland biomes had the lowest K_{max}. Species living in the DES biome had the highest safety, whereas species living in the SMF biome had the lowest safety (Fig. 4b,c).

For individual traits, LMA, VD (including VD, major VD, and minor VD) TLP and π_0, were more aligned with the safety axis than the efficiency axis (Table 2). However, a highly significant proportion of the trade-off residuals were explained by these traits as well, indicating that these traits were associated with departure from the trade-off (Table 2). LMA and VD increased with SR but decreased with MAP. π_0 decreased with SR (positive correlation with absolute values) and TLP increased with MAP (negative correlation with absolute values) (Table S6).

Although there were different slopes among different experimental methods and biomes (Fig. S8; Table S7), we found that for a certain biome, a specific method was mainly used. For example, EFM, PBM, and DRKM methods were mainly used in SMF (81.6%), TS (60%), and woodland/shrubland (59.5%), respectively (Table S7). The deciduous and evergreen plants had similar trendlines, but deciduous species distributed in the bottom right of the trend line, and had higher efficiency but lower safety than evergreen species (Fig. S9).

Discussion

MAP and SR interact to affect the variation in trade-offs at the global scale

Similar to previous studies of branches and leaves, our study demonstrated a significant but weak trade-off between leaf K_{max} and P_{50}, suggesting that the trade-off can be shifted or is not always inevitable (Gleason *et al.*, 2016; Scoffoni & Sack, 2017). We further found that site MAP and SR affected this trade-off. Species living in lower MAP and higher SR conditions had larger trade-off residuals, that is higher safety and efficiency. Higher leaf hydraulic safety is important for plant adaption in dry regions, such as DES biome (Nardini & Luglio, 2014; Scoffoni & Sack, 2017). However, it is also conceivable that higher K_{max} may confer a survival advantage in dry regions (see the Introduction section). Plants living in high SR conditions, for example TS, are subjected to higher leaf temperature and VPD, all else being equal. Such conditions may result in diurnal water stress given the higher evaporative demand and lower turgor pressure under higher light (Kim & Steudle, 2007), which significantly depresses leaf hydraulic conductance, especially at midday (Brodribb & Holbrook, 2004). Indeed, the midday leaf water potential of plants living in TS biome are often lower than leaf P_{50} (Hao *et al.*, 2008). Therefore, high safety is likely important for plants living in high SR conditions. It is possible that higher xylem/leaf hydraulic efficiency could also be beneficial under high light conditions because it may drive higher rates of photosynthesis (high SR), higher (less negative) xylem water potential (Gleason *et al.*, 2012), and lower leaf temperature via evaporative cooling (Scoffoni *et al.*, 2015; Lin *et al.*, 2017).

The combination of MAP and SR revealed significant interactive effects on the trade-off residuals and K_{max}. This is similar to

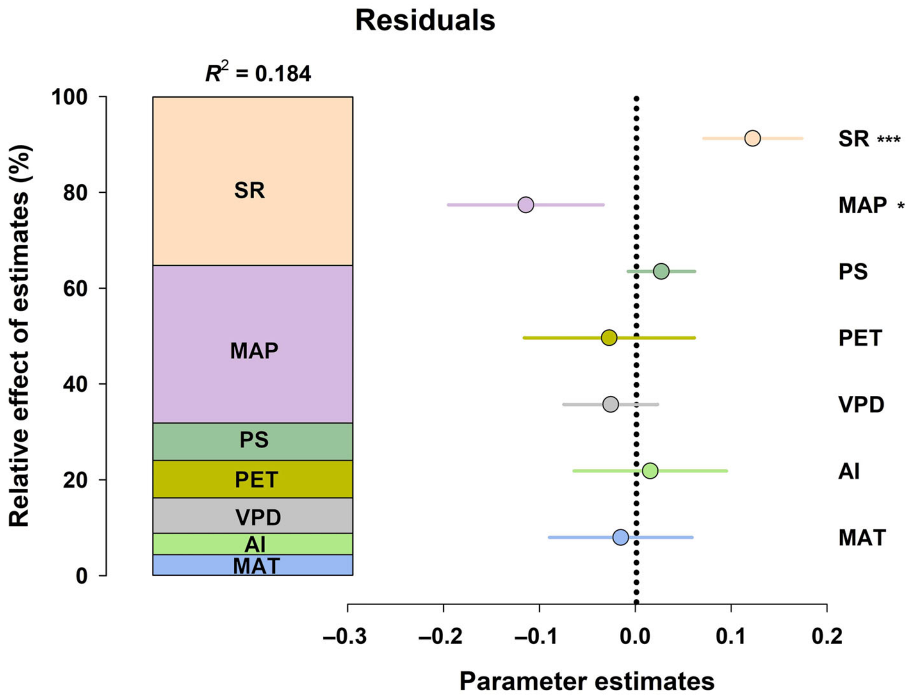

Fig. 2 Relative predictive capacity and significance of the seven climatic variables on the trade-off residuals were estimated using a linear mixed regression model. The relative importance of each factor is quantified as the percentage of absolute value of each parameter estimate (standardized regression coefficients) to the sum of absolute values of all parameter estimates. Averaged parameter estimates of the model predictors are shown with their associated 95% confidence intervals. Climate abbreviations and units follow those in Table 1. Asterisks indicate levels of significance (*, $P < 0.05$; ***, $P < 0.001$).

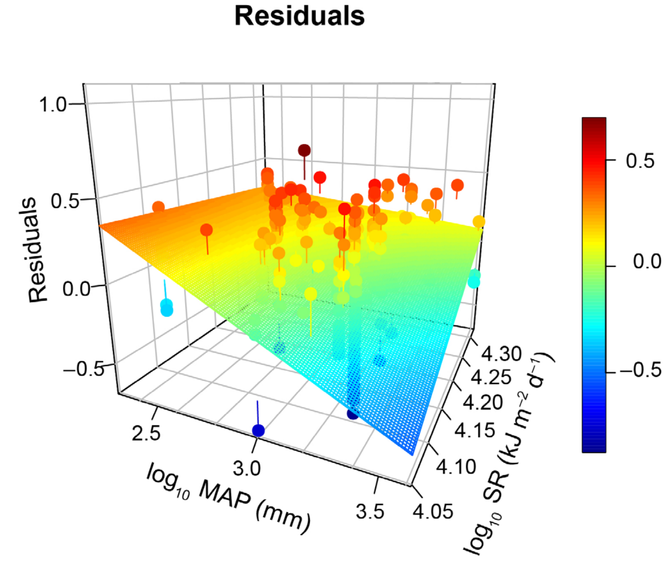

Fig. 3 Predicted interactive effects between mean annual precipitation (MAP) and mean annual solar radiation (SR) on the trade-off residuals. The effects of the interaction between MAP and SR were estimated using a multiple linear mixed regression model (MLMM). The predicted surface of residuals arising from the interaction between MAP and SR resembles a twisted plane, because there was a significant interaction between MAP and SR based on MLMM ($P < 0.05$).

previous claims that irradiance and water conditions may have a combined impact on leaf hydraulic conductance (Guyot *et al.*, 2012; Trifilò *et al.*, 2021). Under low MAP conditions, trade-off residuals were slightly decreased with increasing SR. However, under high MAP conditions, higher SR was associated with positive trade-off residuals (Fig. 3). One possible explanation for this result is that the benefits of higher hydraulic efficiency (higher leaf water potential, photosynthesis, and evaporative cooling) are only possible when SR and water availability are both high (Gleason *et al.*, 2012, 2013; Guyot *et al.*, 2012). Higher K_{leaf} may arise from stronger temperature gradients in the leaf caused by light absorption, which may modify membrane permeabilities, and/or changes in aquaporin expression. However, such enhancement is likely to be achieved only under favorable conditions or mild water stress (Cochard *et al.*, 2006; Guyot *et al.*, 2012; Scoffoni *et al.*, 2018). Therefore, many species living in areas with abundant rainfall but low SR, such as SMF, rainforest, or understory plants, were associated with large negative trade-off residuals (Fig. 4). This may be because many plants in these habitats have low safety requirements, and the low SR in these habitats would result in less transpiration and reduced need for liquid water transport that is keeping the hydraulic supply in balance with demand (Feild *et al.*, 2004; Scoffoni *et al.*, 2016; Liu *et al.*, 2021). A previous unpublished study at the Dinghushan Biosphere Reserve supports this result, where shade-tolerant species had significantly lower efficiency but no difference in safety, compared with light-demanding species (Fig. S10). The clear shifting of the safety–efficiency trade-off across biomes suggests that natural selection and/or species filtering processes have favored different leaf hydraulic strategies in different environments. This may be one possible reason for a weak trade-off at the global scale.

How well are leaf hydraulic efficiency and safety coordinated with other leaf traits?

Six of the seven traits included in our study were more strongly aligned with safety (P_{50}) than efficiency ($K_{\max}$) (Table 2). This

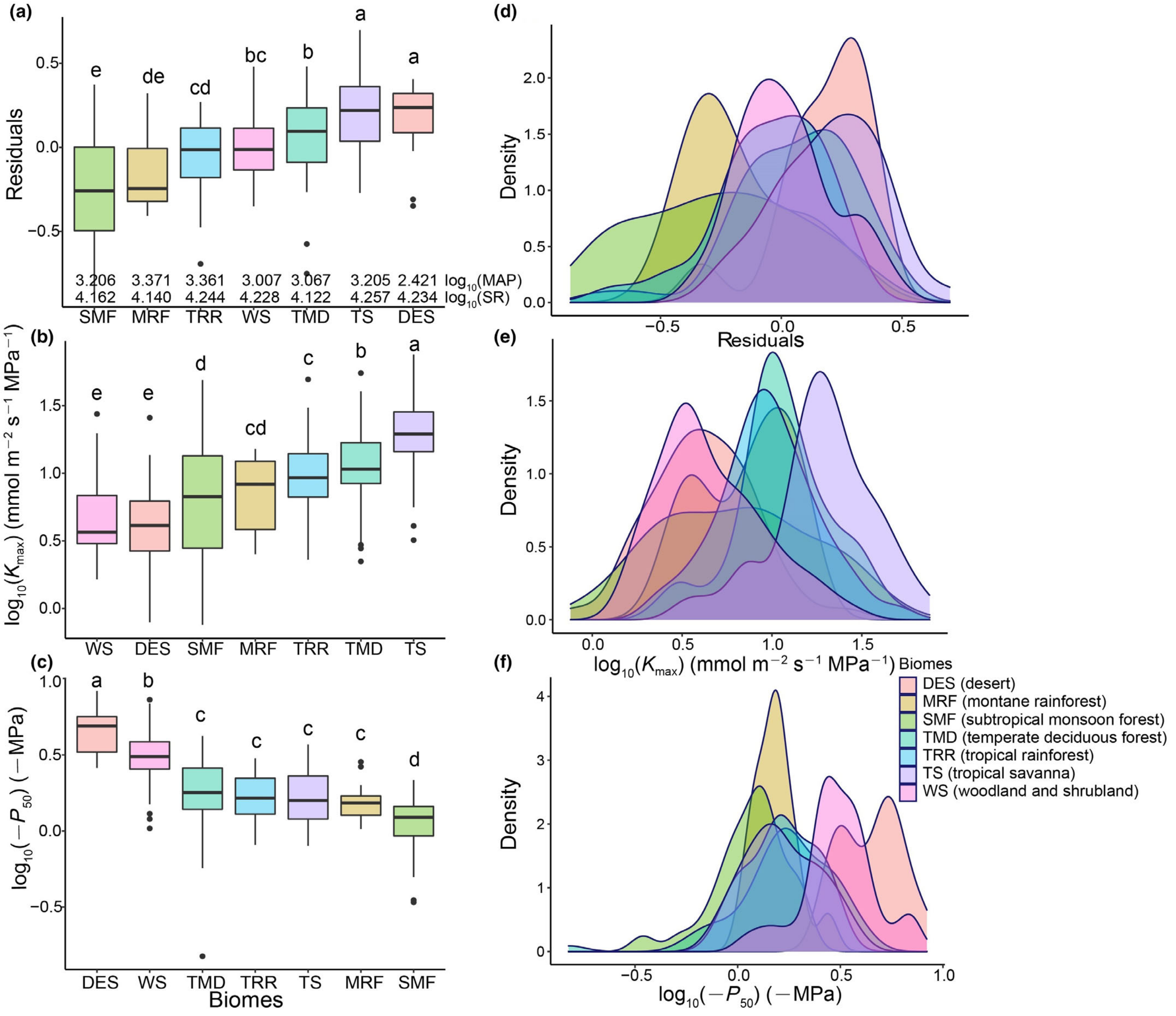

Fig. 4 Variation in the trade-off residuals, leaf hydraulic efficiency (K_{max}), and safety (P_{50}) across seven biomes (left) (a–c). (d–f) Corresponding density distributions among biomes. The mean values of mean annual precipitation (MAP; mm) and solar radiation (SR; kJ m^{-2} d^{-1}) for different biomes are shown in (a). The full name corresponding to each abbreviated biome are shown. The box plots show quartiles for each trait with extreme values as dots, horizontal lines within boxes represent median values. Different letters indicate significant differences among biomes (one-way analysis of variance with LSD test, $P < 0.05$).

result was similar to a recent study of seven species with widely ranging drought tolerance, where VD and mesophyll anatomy traits were unrelated to K_{max}, but were correlated with P_{50} (Xiong & Flexas, 2022). This result supports the idea that leaf hydraulic efficiency and safety are not always linked, in either the xylem or extraxylary components (Blackman *et al.*, 2010; Xiong & Flexas, 2022). In addition, K_{leaf} is affected by multiple anatomical/biochemical factors (Scoffoni *et al.*, 2016), and some of these factors affect K_{leaf} conjunctly. For example, VD (apoplastic pathway) and aquaporin activity (symplastic pathway) both affect water flux across the bundle sheath to the mesophyll. However, the negative effect of low VD on K_{leaf} can be compensated for by an increase in aquaporin activity (Harayama *et al.*, 2019). Additionally, plants with higher minor VD almost always have thinner veins and conduits, resulting in lower leaf hydraulic efficiency (Nardini *et al.*, 2012; Feild & Brodribb, 2013). Therefore, from the perspective of leaf anatomical traits, we should probably not expect an inevitable trade-off between K_{max} and P_{50}.

We further found that plants with high LMA and VD, and low TLP and π_0 generally live under conditions with low MAP and/or high SR (Table S6). This is consistent with a previous report that TLP and π_0 are good predictors of plant distribution across water availability gradients (Bartlett *et al.*, 2012). Similarly, LMA and VD increased with irradiance but decreased with

Table 2 Fit static of the third variable (leaf traits), after including leaf hydraulic efficiency (K_{max}) and safety (P_{50}) in a linear multiple regression model.

	R^2 $\log_{10}(K_{max})$	P	R^2 $\log_{10}(-P_{50})$	P	R^2 residuals	P	n
$\log_{10}$(LMA)	0.012	0.395	**0.309**	**< 0.001**	**0.12**	**< 0.001**	195
$\log_{10}$(−TLP)	0.012	0.056	**0.267**	**< 0.001**	**0.153**	**< 0.001**	167
$\log_{10}$(VD)	0.01	0.939	**0.328**	**< 0.001**	**0.228**	**< 0.001**	74
$\log_{10}(\varepsilon)$	0.061 (−)	0.093	0.072	0.071	0	0.92	43
$\log_{10}(-\pi_0)$	**0.088**	**0.017**	**0.15**	**0.001**	**0.24**	**< 0.001**	66
$\log_{10}$(minor VD)	0.048 (−)	0.204	**0.209**	**< 0.001**	**0.133**	**0.003**	65
$\log_{10}$(major VD)	0.01	0.659	**0.35**	**< 0.001**	**0.26**	**< 0.001**	65

Coefficient of determination values (R^2) for K_{max} and P_{50} represent the portion of explained variation attributable to K_{max} and P_{50}. The R^2 of residuals represents the portion of explained variation that is attributable to the third variable. The negative sign in parentheses indicates negative correlation. Bold font denotes significant relationships. The third variable (leaf traits) abbreviations and units follow those in Table 1.

water availability, which has been reported previously (Poorter *et al.*, 2009; Sack & Scoffoni, 2013). Thus, the additional carbon investment associated with higher LMA and VD may enable plants to achieve higher safety and efficiency in low MAP and high SR habitats.

High diversity of leaf hydraulic strategies across biomes

Our results suggest that much of the unexplained variation in the trade-off cannot be accounted for by climate factors. One possible explanation for this is that leaf hydraulic traits are highly variable within biomes. In support of this hypothesis, we found a large overlap of K_{max}, P_{50}, and trade-off residuals among biomes (Fig. 4d–f). This is especially evident for K_{max}, which is more mutable, relative to P_{50} (Fig. S11). A possible explanation for this wide variation in K_{max} that extraxylary leaf hydraulic conductance is likely elastic and responsive to internal and external conditions, enabling plants to avoid embolism but also allowing for the quick upregulation of water transport when leaf water status is favorable (Scoffoni *et al.*, 2023). Therefore, we might also expect leaf hydraulic conductance to change with leaf age, damage, and microclimates (Sack & Holbrook, 2006). The study at the Dinghushan Biosphere Reserve also supports the premise that differences in shade tolerance among co-occurring species, as explained by SR alignment with K_{max} and trade-off residuals, may engender niche differentiation. Although other adaptive strategies, such as leaf shedding, may allow plants to exhibit much variation in safety under similar conditions or even in drier environments (Choat *et al.*, 2012), our study showed that deciduous species shared the same trendline with evergreen species (Fig. S9), suggesting that deciduousness did not modify the trade-off. Rather, deciduous species were located along the same trendline, but in the region of the function where hydraulic efficiency was high, but at the expense of hydraulic safety.

A possible limitation of our study is that we cannot completely rule out the influence of different methods on the trade-off, but we think these differences have had only a minor influence on our results. Previous studies have demonstrated that differences among K_{leaf} methods (e.g. EFM, DRKM, or HPFM) and P_{50} methods (e.g. using EFM or DRKM) were relatively small within species as compared to the differences across species and biomes (Sack *et al.*, 2002; Hernandez-Santana *et al.*, 2016; Trifilo *et al.*, 2016). Some researchers have found that using RKM may overestimate K_{max} and P_{50} in some cases (e.g. compared with measurements of DRKM and EFM) (Brodribb & Holbrook, 2006; Scoffoni *et al.*, 2008; Blackman & Brodribb, 2011). In the present study, we found that the trade-off residuals measured using RKM differed from those using other methods in only two biomes. For example, the trade-off residuals measured using RKM were larger than EFM in the SMF biome but lower than DRKM in the DES biome (Fig. S12). However, importantly, these different methods resulted in similar trade-off residuals in all other biomes. If differences in trade-off residuals had arisen solely from the methods used, we should expect these methods to bias the residuals in the same way (direction and magnitude) in all cases, but this is not what happened. Therefore, the differences in trendlines among methods were most likely due to differences among biomes (Table S7). This suggests that we would have arrived at similar conclusions even if the same method had been used in all cases.

Conclusion

In summary, our study showed the evidence of a safety–efficiency trade-off in leaves at the global scale. However, the revealed trade-off was markedly weak, with safety and efficiency varying largely independently of one another across species. Nevertheless, significant portions of explained and unexplained variation in the safety–efficiency trade-off suggest that these two physiologically important traits are likely linked together, and this linkage can be effectively modified via VD, osmotic regulation, LMA, and climate. These differences in leaf traits and climate across species and habitats were associated with meaningful shifts in this trade-off, which would seemingly allow for a wide diversity of hydraulic strategies, thus engendering plant success across the world's terrestrial habitats.

Acknowledgements

We are grateful to the editor and reviewers for their constructive suggestions and comments on earlier versions of this manuscript. This work was supported by the National Natural Science Foundation of China (U23A20156, 32371575), the Guangdong Basic and Applied Basic Research Foundation (2024B1515020067), the Guangdong Science and Technology Plan Project (2023B1212060046), and the Youth Innovation Promotion Association of the Chinese Academy of Sciences (Y2023093).

Competing interests

None declared.

Author contributions

YJ and QY designed this work. YJ, XL and PH performed the measurements for species in the Dinghushan Biosphere Reserve, which was supported by QY. YJ, HL, XL and PH collected data from previous studies. YJ, HL, XL and SMG contributed to data analysis and interpretation. YJ wrote the first draft of the manuscript with inputs from PH, X-YL and GW. QY, XL, HL and SMG made valuable contributions to subsequent drafts of the manuscript.

ORCID

Sean M. Gleason https://orcid.org/0000-0002-5607-4741
Pengcheng He https://orcid.org/0000-0001-9531-531X
Yi Jin https://orcid.org/0000-0001-9024-4882
Xingyun Liang https://orcid.org/0009-0002-6318-2019
Hui Liu https://orcid.org/0000-0003-4027-499X
Xiaorong Liu https://orcid.org/0000-0001-5366-7739
Qing Ye https://orcid.org/0000-0001-5445-0996

Data availability

The data that support the findings of this study are available at Dataset S1 in the Supporting Information.

References

Abatzoglou JT, Dobrowski SZ, Parks SA, Hegewisch KC. 2018. TerraClimate, a high-resolution global dataset of monthly climate and climatic water balance from 1958–2015. *Scientific Data* **5**: 170191.

Bartlett MK, Scoffoni C, Sack L. 2012. The determinants of leaf turgor loss point and prediction of drought tolerance of species and biomes: a global meta-analysis. *Ecology Letters* **15**: 393–405.

Bates D, Mächler M, Bolker B, Walker S. 2015. Fitting linear mixed-effects models using LME4. *Journal of Statistical Software* **67**: 1–48.

Bi M, Jiang C, Yao G, Turner NC, Scoffoni C, Fang X. 2023. Rapid drought-recovery of gas exchange in *Caragana* species adapted to low mean annual precipitation. *Plant, Cell & Environment* **46**: 2296–2309.

Bittencourt PRL, Pereira L, Oliveira RS. 2016. On xylem hydraulic efficiencies, wood space-use and the safety–efficiency tradeoff. *New Phytologist* **211**: 1152–1155.

Blackman CJ, Brodribb TJ. 2011. Two measures of leaf capacitance: insights into the water transport pathway and hydraulic conductance in leaves. *Functional Plant Biology* **38**: 118–126.

Blackman CJ, Brodribb TJ, Jordan GJ. 2010. Leaf hydraulic vulnerability is related to conduit dimensions and drought resistance across a diverse range of woody angiosperms. *New Phytologist* **188**: 1113–1123.

Blackman CJ, Brodribb TJ, Jordan GJ. 2012. Leaf hydraulic vulnerability influences species' bioclimatic limits in a diverse group of woody angiosperms. *Oecologia* **168**: 1–10.

Blackman CJ, Gleason SM, Chang Y, Cook AM, Laws C, Westoby M. 2014. Leaf hydraulic vulnerability to drought is linked to site water availability across a broad range of species and climates. *Annals of Botany* **114**: 435–440.

Blackman CJ, Halliwell B, Hartill GE, Brodribb TJ. 2024. Petiole XLA (xylem to leaf area ratio) integrates hydraulic safety and efficiency across a diverse group of eucalypt leaves. *Plant, Cell & Environment* **47**: 49–58.

Brodersen CR. 2016. Finding support for theoretical tradeoffs in xylem structure and function. *New Phytologist* **209**: 8–10.

Brodribb TJ, Holbrook NM. 2004. Diurnal depression of leaf hydraulic conductance in a tropical tree species. *Plant, Cell & Environment* **27**(7): 820–827.

Brodribb TJ, Bienaimé D, Marmottant P. 2016. Revealing catastrophic failure of leaf networks under stress. *Proceedings of the National Academy of Sciences, USA* **113**: 4865–4869.

Brodribb TJ, Feild TS, Jordan GJ. 2007. Leaf maximum photosynthetic rate and venation are linked by hydraulics. *Plant Physiology* **144**: 1890–1898.

Brodribb TJ, Holbrook NM. 2003. Stomatal closure during leaf dehydration, correlation with other leaf physiological traits. *Plant Physiology* **132**: 2166–2173.

Brodribb TJ, Holbrook NM. 2006. Declining hydraulic efficiency as transpiring leaves desiccate: two types of response. *Plant, Cell & Environment* **29**: 2205–2215.

Bucci SJ, Carbonell Silletta LM, Garré A, Cavallaro A, Efron ST, Arias NS, Goldstein G, Scholz FG. 2019. Functional relationships between hydraulic traits and the timing of diurnal depression of photosynthesis. *Plant, Cell & Environment* **42**: 1603–1614.

Bucci SJ, Scholz FG, Peschuiutta ML, Arias NS, Meinzer FC, Goldstein G. 2013. The stem xylem of Patagonian shrubs operates far from the point of catastrophic dysfunction and is additionally protected from drought-induced embolism by leaves and roots. *Plant, Cell & Environment* **36**: 2163–2174.

Buckley TN, John GP, Scoffoni C, Sack L. 2015. How does leaf anatomy influence water transport outside the xylem? *Plant Physiology* **168**: 1616–1635.

Choat B, Jansen S, Brodribb TJ, Cochard H, Delzon S, Bhaskar R, Bucci SJ, Feild TS, Gleason SM, Hacke UG *et al.* 2012. Global convergence in the vulnerability of forests to drought. *Nature* **491**: 752–755.

Cochard H, Venisse J-S, Barigah TS, Brunel N, Herbette S, Guilliot A, Tyree MT, Sakr S. 2006. Putative role of aquaporins in variable hydraulic conductance of leaves in response to light. *Plant Physiology* **143**: 122–133.

Duursma R, Choat B. 2017. FITPLC – an R package to fit hydraulic vulnerability curves. *Journal of Plant Hydraulics* **4**: e002.

Feild TS, Arens NC, Doyle JA, Dawson TE, Donoghue MJ. 2004. Dark and disturbed: a new image of early angiosperm ecology. *Paleobiology* **30**: 82–107.

Feild TS, Brodribb TJ. 2013. Hydraulic tuning of vein cell microstructure in the evolution of angiosperm venation networks. *New Phytologist* **199**: 720–726.

Fick SE, Hijmans RJ. 2017. WorldClim 2: new 1-km spatial resolution climate surfaces for global land areas. *International Journal of Climatology* **37**: 4302–4315.

Franks PJ. 2006. Higher rates of leaf gas exchange are associated with higher leaf hydrodynamic pressure gradients. *Plant, Cell & Environment* **29**: 584–592.

García-Palacios P, Gross N, Gaitán J, Maestre FT. 2018. Climate mediates the biodiversity–ecosystem stability relationship globally. *Proceedings of the National Academy of Sciences, USA* **115**: 8400–8405.

Gleason SM, Butler DW, Waryszak P. 2013. Shifts in leaf and stem hydraulic traits across aridity gradients in eastern Australia. *International Journal of Plant Sciences* **174**: 1292–1301.

Gleason SM, Butler DW, Ziemińska K, Waryszak P, Westoby M. 2012. Stem xylem conductivity is key to plant water balance across Australian angiosperm species. *Functional Ecology* **26**: 343–352.

Gleason SM, Westoby M, Jansen S, Choat B, Hacke UG, Pratt RB, Bhaskar R, Brodribb TJ, Bucci SJ, Cao K-F *et al.* 2016. Weak tradeoff between xylem safety and xylem-specific hydraulic efficiency across the world's woody plant species. *New Phytologist* **209**: 123–136.

Grömping U. 2006. Relative importance for linear regression in R: the package RELAIMPO. *Journal of Statistical Software* **17**: 1–27.

Grubb PJ. 1998. A reassessment of the strategies of plants which cope with shortages of resources. *Perspectives in Plant Ecology, Evolution and Systematics* **1**: 3–31.

Guyot G, Scoffoni C, Sack L. 2012. Combined impacts of irradiance and dehydration on leaf hydraulic conductance: insights into vulnerability and stomatal control. *Plant, Cell & Environment* **35**: 857–871.

Hao GY, Hoffmann WA, Scholz FG, Bucci SJ, Meinzer FC, Franco AC, Cao K, Goldstein G. 2008. Stem and leaf hydraulics of congeneric tree species from adjacent tropical savanna and forest ecosystems. *Oecologia* **155**: 405–415.

Harayama H, Kitao M, Agathokleous E, Ishida A. 2019. Effects of major vein blockage and aquaporin inhibition on leaf hydraulics and stomatal conductance. *Proceedings of the Royal Society B: Biological Sciences* **286**: 20190799.

He P, Gleason SM, Wright IJ, Weng E, Liu H, Zhu S, Lu M, Luo Q, Li R, Wu G *et al.* 2020. Growing-season temperature and precipitation are independent drivers of global variation in xylem hydraulic conductivity. *Global Change Biology* **26**: 1833–1841.

Hernandez-Santana V, Rodriguez-Dominguez CM, Fernández JE, Diaz-Espejo A. 2016. Role of leaf hydraulic conductance in the regulation of stomatal conductance in almond and olive in response to water stress. *Tree Physiology* **36**: 725–735.

Holloway-Phillips M-M, Brodribb TJ. 2011. Minimum hydraulic safety leads to maximum water-use efficiency in a forage grass. *Plant, Cell & Environment* **34**: 302–313.

Huang R, Di N, Xi B, Yang J, Duan J, Li X, Feng J, Choat B, Tissue D. 2024. Herb hydraulics: variation and correlation for traits governing drought tolerance and efficiency of water transport. *Science of the Total Environment* **907**: 168095.

Huo J, Shi Y, Chen J, Zhang H, Feng L, Zhao Y, Zhang Z. 2022. Hydraulic trade-off and coordination strategies mediated by leaf functional traits of desert shrubs. *Frontiers in Plant Science* **13**: 938758.

Isasa E, Link RM, Jansen S, Tezeh FR, Kaack L, Sarmento Cabral J, Schuldt B. 2023. Addressing controversies in the xylem embolism resistance–vessel diameter relationship. *New Phytologist* **238**: 283–296.

John GP, Scoffoni C, Buckley TN, Villar R, Poorter H, Sack L. 2017. The anatomical and compositional basis of leaf mass per area. *Ecology Letters* **20**: 412–425.

Kim YX, Steudle E. 2007. Light and turgor affect the water permeability (aquaporins) of parenchyma cells in the midrib of leaves of *Zea mays*. *Journal of Experimental Botany* **58**: 4119–4129.

Lens F, Gleason SM, Bortolami G, Brodersen C, Delzon S, Jansen S. 2022. Functional xylem characteristics associated with drought-induced embolism in angiosperms. *New Phytologist* **236**: 2019–2036.

Lens F, Sperry JS, Christman MA, Choat B, Rabaey D, Jansen S. 2011. Testing hypotheses that link wood anatomy to cavitation resistance and hydraulic conductivity in the genus *Acer*. *New Phytologist* **190**: 709–723.

Lin H, Chen Y, Zhang H, Fu P, Fan Z. 2017. Stronger cooling effects of transpiration and leaf physical traits of plants from a hot dry habitat than from a hot wet habitat. *Functional Ecology* **31**: 2202–2211.

Liu H, Ye Q, Gleason SM, He P, Yin D. 2021. Weak tradeoff between xylem hydraulic efficiency and safety: climatic seasonality matters. *New Phytologist* **229**: 1440–1452.

Martorell S, Medrano H, Tomàs M, Escalona JM, Flexas J, Diaz-Espejo A. 2015. Plasticity of vulnerability to leaf hydraulic dysfunction during acclimation to drought in grapevines: an osmotic-mediated process. *Physiologia Plantarum* **153**: 381–391.

McKown AD, Cochard H, Sack L. 2010. Decoding leaf hydraulics with a spatially explicit model: principles of venation architecture and implications for its evolution. *The American Naturalist* **175**: 447–460.

Nardini A, Luglio J. 2014. Leaf hydraulic capacity and drought vulnerability: possible trade-offs and correlations with climate across three major biomes. *Functional Ecology* **28**: 810–818.

Nardini A, Õunapuu-Pikas E, Savi T. 2014. When smaller is better: leaf hydraulic conductance and drought vulnerability correlate to leaf size and venation density across four *Coffea arabica* genotypes. *Functional Plant Biology* **41**: 972–982.

Nardini A, Pedà G, Rocca NL. 2012. Trade-offs between leaf hydraulic capacity and drought vulnerability: morpho-anatomical bases, carbon costs and ecological consequences. *New Phytologist* **196**: 788–798.

Ocheltree TW, Nippert JB, Prasad PV. 2016. A safety vs efficiency trade-off identified in the hydraulic pathway of grass leaves is decoupled from photosynthesis, stomatal conductance and precipitation. *New Phytologist* **210**: 97–107.

Poorter H, Niinemets Ü, Poorter L, Wright IJ, Villar R. 2009. Causes and consequences of variation in leaf mass per area (LMA): a meta-analysis. *New Phytologist* **182**: 565–588.

Reich PB. 2014. The world-wide 'fast–slow' plant economics spectrum: a traits manifesto. *Journal of Ecology* **102**: 275–301.

Sack L, Dietrich EM, Streeter CM, Sánchez-Gómez D, Holbrook NM. 2008. Leaf palmate venation and vascular redundancy confer tolerance of hydraulic disruption. *Proceedings of the National Academy of Sciences, USA* **105**: 1567–1572.

Sack L, Frole K. 2006. Leaf structural diversity is related to hydraulic capacity in tropical rain forest trees. *Ecology* **87**: 483–491.

Sack L, Holbrook MN. 2006. Leaf hydraulics. *Annual Review of Plant Biology* **57**: 361–381.

Sack L, Melcher PJ, Zwieniecki MA, Holbrook NM. 2002. The hydraulic conductance of the angiosperm leaf lamina: a comparison of three measurement methods. *Journal of Experimental Botany* **53**: 2177–2184.

Sack L, Scoffoni C. 2012. Measurement of leaf hydraulic conductance and stomatal conductance and their responses to irradiance and dehydration using the evaporative flux method (EFM). *Journal of Visualized Experiments* **70**: e4179.

Sack L, Scoffoni C. 2013. Leaf venation: structure, function, development, evolution, ecology and applications in the past, present and future. *New Phytologist* **198**: 983–1000.

Sack L, Scoffoni C, John GP, Poorter H, Mason CM, Mendez-Alonzo R, Donovan LA. 2013. How do leaf veins influence the worldwide leaf economic spectrum? Review and synthesis. *Journal of Experimental Botany* **64**: 4053–4080.

Sack L, Tyree MT, Holbrook NM. 2005. Leaf hydraulic architecture correlates with regeneration irradiance in tropical rainforest trees. *New Phytologist* **167**: 403–413.

Schenk HJ, Espino S, Rich-Cavazos SM, Jansen S. 2018. From the sap's perspective: the nature of vessel surfaces in angiosperm xylem. *American Journal of Botany* **105**: 172–185.

Schenk HJ, Steppe K, Jansen S. 2015. Nanobubbles: a new paradigm for air-seeding in xylem. *Trends in Plant Science* **20**: 199–205.

Scoffoni C, Albuquerque C, Brodersen CR, Townes SV, John GP, Cochard H, Buckley TN, McElrone AJ, Sack L. 2017. Leaf vein xylem conduit diameter influences susceptibility to embolism and hydraulic decline. *New Phytologist* **213**: 1076–1092.

Scoffoni C, Albuquerque C, Buckley TN, Sack L. 2023. The dynamic multi-functionality of leaf water transport outside the xylem. *New Phytologist* **239**: 2099–2107.

Scoffoni C, Albuquerque C, Cochard H, Buckley TN, Fletcher LR, Caringella MA, Bartlett M, Brodersen CR, Jansen S, McElrone AJ *et al.* 2018. The causes of leaf hydraulic vulnerability and its influence on gas exchange in *Arabidopsis thaliana*. *Plant Physiology* **178**: 1584–1601.

Scoffoni C, Chatelet DS, Pasquet-kok J, Rawls M, Donoghue MJ, Edwards EJ, Sack L. 2016. Hydraulic basis for the evolution of photosynthetic productivity. *Nature Plants* **2**: 16072.

Scoffoni C, Kunkle J, Pasquet-Kok J, Vuong C, Patel AJ, Montgomery RA, Givnish TJ, Sack L. 2015. Light-induced plasticity in leaf hydraulics, venation, anatomy, and gas exchange in ecologically diverse *Hawaiian lobeliads*. *New Phytologist* **207**: 43–58.

Scoffoni C, McKown AD, Rawls M, Sack L. 2011a. Dynamics of leaf hydraulic conductance with water status: quantification and analysis of species differences under steady state. *Journal of Experimental Botany* **63**: 643–658.

Scoffoni C, Pou A, Aasamaa K, Sack L. 2008. The rapid light response of leaf hydraulic conductance: new evidence from two experimental methods. *Plant, Cell & Environment* **31**: 1803–1812.

Scoffoni C, Rawls M, McKown AD, Cochard H, Sack L. 2011b. Decline of leaf hydraulic conductance with dehydration: relationship to leaf size and venation architecture. *Plant Physiology* **156**: 832–843.

Scoffoni C, Sack L. 2017. The causes and consequences of leaf hydraulic decline with dehydration. *Journal of Experimental Botany* **68**: 4479–4496.

Scoffoni C, Vuong C, Diep S, Cochard H, Sack L. 2014. Leaf shrinkage with dehydration: coordination with hydraulic vulnerability and drought tolerance. *Plant Physiology* **164**: 1772–1788.

Trifilò P, Petruzzellis F, Abate E, Nardini A. 2021. The extra-vascular water pathway regulates dynamic leaf hydraulic decline and recovery in *Populus nigra*. *Physiologia Plantarum* **172**: 29–40.

Trifilo P, Raimondo F, Savi T, Lo Gullo MA, Nardini A. 2016. The contribution of vascular and extra-vascular water pathways to drought-induced decline of leaf hydraulic conductance. *Journal of Experimental Botany* **67**: 5029–5039.

Tyree MT, Zimmermann MH. 2002. *Xylem structure and the ascent of sap*. Berlin, Germany: Springer-Verlag.

Warton DI, Duursma RA, Falster DS, Taskinen S. 2012. SMATR 3 – an R package for estimation and inference about allometric lines. *Methods in Ecology and Evolution* **3**: 257–259.

Whittaker RH. 1975. *Communities and ecosystems, 2nd revise edn*. New York, NY, USA: MacMillan.

Wickham H. 2016. *GGPLOT2: elegant graphics for data analysis*. New York, NY, USA: Springer-Verlag.

Xiong D, Flexas J. 2022. Safety–efficiency tradeoffs? Correlations of photosynthesis, leaf hydraulics, and dehydration tolerance across species. *Oecologia* **200**: 51–64.

Xiong D, Yu T, Zhang T, Li Y, Peng S, Huang J. 2014. Leaf hydraulic conductance is coordinated with leaf morpho-anatomical traits and nitrogen status in the genus *Oryza*. *Journal of Experimental Botany* **66**: 741–748.

Yan C, Ni M, Cao K, Zhu S. 2020. Leaf hydraulic safety margin and safety-efficiency trade-off across angiosperm woody species. *Biology Letters* **16**: 20200456.

Yao G, Nie Z, Turner NC, Li F, Gao T, Fang X, Scoffoni C. 2021. Combined high leaf hydraulic safety and efficiency provides drought tolerance in *Caragana* species adapted to low mean annual precipitation. *New Phytologist* **229**: 230–244.

Zhang Q, Zhu S, Jansen S, Cao K. 2021. Topography strongly affects drought stress and xylem embolism resistance in woody plants from a karst forest in Southwest China. *Functional Ecology* **35**: 566–577.

Zhang X, Ma S, Hu H, Li F, Bao W, Huang L. 2024. A trade-off between leaf hydraulic efficiency and safety across three xerophytic species in response to increased rock fragment content. *Tree Physiology* **44**: tpae010.

Zhu S, Chen Y, Ye Q, He P, Liu H, Li R, Fu P, Jiang G, Cao K. 2018. Leaf turgor loss point is correlated with drought tolerance and leaf carbon economics traits. *Tree Physiology* **38**: 658–663.

Zimmermann M. 1983. *Xylem structure and the ascent of sap*. Berlin, Germany: Springer-Verlag.

Zomer RJ, Trabucco A, Bossio DA, Verchot LV. 2008. Climate change mitigation: a spatial analysis of global land suitability for clean development mechanism afforestation and reforestation. *Agriculture, Ecosystems & Environment* **126**: 67–80.

Supporting Information

Additional Supporting Information may be found online in the Supporting Information section at the end of the article.

Dataset S1 The data that supports the findings of this study.

Fig. S1 Map of all 81 study sites against the mean annual precipitation and sites plotted onto in Whittaker's biomes diagram.

Fig. S2 Principal component analysis on the 280 trade-off residual observations based on seven climatic variables.

Fig. S3 Relative predictive capacity of the seven climatic variables on leaf hydraulic efficiency ($K_{\max}$) and safety (P_{50}).

Fig. S4 Relationships between leaf hydraulic efficiency ($K_{\max}$) and safety (P_{50}) across regions with different mean annual precipitation and mean annual solar radiation.

Fig. S5 Trade-off residuals in relation to mean annual precipitation under different solar radiation conditions and to SR under different MAP conditions.

Fig. S6 Predicted interactive effects between mean annual precipitation and mean annual solar radiation on leaf hydraulic efficiency ($K_{\max}$) and safety (P_{50}).

Fig. S7 Leaf hydraulic efficiency ($K_{\max}$) and safety (P_{50}) in relation to mean annual precipitation under different solar radiation conditions and to SR under different MAP conditions.

Fig. S8 Relationships between leaf hydraulic efficiency ($K_{\max}$) and safety (P_{50}) across biomes.

Fig. S9 Relationships between leaf hydraulic efficiency ($K_{\max}$) and safety (P_{50}) in different leaf types (evergreen and deciduous).

Fig. S10 Difference in leaf hydraulic efficiency ($K_{\max}$) and safety (P_{50}) for light-demanding and shade-tolerant species that were studied in the Dinghushan Biosphere Reserve.

Fig. S11 Coefficient of variation in leaf hydraulic efficiency ($K_{\max}$) and safety (P_{50}) across biomes.

Fig. S12 Comparing the differences in trade-off residuals within the same biome measured using different methods.

Notes S1 Published references from which data were extracted for analyses.

Table S1 Correlations among the seven climate variables examined in our study. Correlation coefficients are given.

Table S2 The trade-off residual trends in relation to seven individual climate variables.

Table S3 Leaf hydraulic efficiency ($K_{\max}$) and safety (P_{50}) trends in relation to seven individual climate variables.

Table S4 Relationships between log-transformed leaf hydraulic efficiency ($K_{\max}$) and safety (P_{50}) across regions with different mean annual precipitation.

Table S5 Relationships between leaf hydraulic efficiency ($K_{\max}$) and safety (P_{50}) across regions with different mean annual solar radiation.

Table S6 Correlations of leaf traits with mean annual solar radiation and mean annual precipitation.

Table S7 Relationships between leaf hydraulic efficiency ($K_{\max}$) and safety (P_{50}) among methods.